

# Soft-mode behavior of electromagnons in multiferroic manganite

A. M. Shuvaev,<sup>1</sup> J. Hemberger,<sup>2</sup> D. Niermann,<sup>2</sup> F. Schrettle,<sup>3</sup> A. Loidl,<sup>3</sup>  
V. Yu. Ivanov,<sup>4</sup> V. D. Travkin,<sup>4</sup> A. A. Mukhin,<sup>4</sup> and A. Pimenov<sup>1</sup>

<sup>1</sup>*Experimentelle Physik IV, Universität Würzburg, 97074 Würzburg, Germany*

<sup>2</sup>*II. Physikalisches Institut, Universität zu Köln, 50937 Köln, Germany*

<sup>3</sup>*Experimentalphysik V, EKM, Universität Augsburg, 86135 Augsburg, Germany*

<sup>4</sup>*General Physics Institute, Russian Acad. Sci., 119991 Moscow, Russia*

(Dated: October 17, 2018)

The behavior of the low-frequency electromagnon in multiferroic DyMnO<sub>3</sub> has been investigated in external magnetic fields and in a magnetically ordered state. Significant softening of the electromagnon frequency is observed for external magnetic fields parallel to the *a*-axis ( $B\parallel a$ ), revealing a number of similarities to a classical soft mode behavior known for ferroelectric phase transitions. The softening of the electromagnon yields an increase of the static dielectric permittivity which follows a similar dependence as predicted by the Lyddane-Sachs-Teller relation. Within the geometry  $B\parallel b$  the increase of the electromagnon intensity does not correspond to the softening of the eigenfrequency. In this case the increase of the static dielectric permittivity seem to be governed by the motion of the domain walls.

## INTRODUCTION

Soft modes have long been studied in connection with structural phase transitions in crystalline solids [1–3]. Close to such phase transition the frequency of the normally lowest lattice vibration strongly decreases [4] (softens) as a result of a "flattening" of an effective potential. Therefore, soft modes reflect an instability of the crystal lattice [5] and are often accompanied by a substantial nonlinearity of the system. Especially in ferroelectric crystals the softening of a lattice vibration is followed by a divergence of the static dielectric permittivity. In a simple case a lattice vibration can be written in the Lorentz form,

$$\varepsilon(\omega) = \varepsilon_\infty + \frac{\Delta\varepsilon \cdot \omega_r^2}{\omega_r^2 - \omega^2 - i\omega\gamma} = \varepsilon_\infty \frac{\omega_{LO}^2 - \omega^2 - i\omega\gamma}{\omega_r^2 - \omega^2 - i\omega\gamma}. \quad (1)$$

Here  $\omega_r$  is the resonance frequency,  $\omega_{LO}$  is the frequency of the longitudinal phonon,  $\gamma$  is the damping,  $\varepsilon_\infty$  is the high frequency permittivity, and  $\Delta\varepsilon$  is the dielectric contribution of the mode to the static dielectric permittivity. From this equation the well known Lyddane-Sachs-Teller (LST) relation immediately follows [3]

$$\varepsilon(0)/\varepsilon_\infty = (\varepsilon_\infty + \Delta\varepsilon)/\varepsilon_\infty = [\omega_{LO}/\omega_r]^2. \quad (2)$$

Close to structural phase transition in ferroelectrics  $\omega_r$  softens and  $\omega_{LO}$  basically remains constant [1], which leads to the mentioned divergence of the static dielectric permittivity.

Physically similar conclusion can be drawn taking into account that the spectral weight of a single excitation is often conserved. In spectroscopy this is generally termed as a sum rule and can be derived from first principles [6]. The spectral weight is proportional to the electron density and can be written as  $S \sim \Delta\varepsilon \cdot \omega_r^2$ . Evidently, in order to preserve the constant spectral weight with decreasing resonance frequency, the dielectric contribution

must diverge as  $\Delta\varepsilon \sim 1/\omega_r^2$ . The last formula works well for the soft lattice vibrations and represents another form of the LST relation.

Although governed by different mechanisms, qualitatively similar effects can be observed in glassy materials as well. In this case a broad structural relaxation mode, called alpha-relaxation [7], moves towards zero frequency reflecting the freezing of the ionic movement. Contrary to the crystalline solids, in glasses the situation is more complicated and the spectral weight of the structural relaxation is not conserved. However, the divergence of the static dielectric constant close to glass transition has been put into discussion for non-crystalline solids as well [8].

Another sum rule can be derived in case of dielectric spectroscopy, which of course correlates with the conservation of the spectral weight. This sum rule states that the static dielectric permittivity can be calculated as a sum of all contributions from absorption processes at finite frequencies [6]. Therefore, in experiment one might try to always correlate the changes in static properties with changes in the absorption spectra at finite frequencies. As a characteristic example, the suppression of an electro-active mode in multiferroic GdMnO<sub>3</sub> and TbMnO<sub>3</sub> has been put forward as a spectroscopic explanation of field induced changes in the static dielectric constant [9].

Multiferroics represent an intriguing class of materials in which electric and magnetic orders coexist [10–12]. Most interesting effects occur if both orders are strongly coupled. This leads to such effects like the control of electric polarization by external magnetic field or the control of magnetization by electric field. In addition to static polarization, dynamic properties of multiferroics are very rich and in various compounds show the existence of a series of new excitations. These excitations are electrically active magnetic modes of the cycloidal spin structure and they have been called electromagnons [13, 14].

The electromagnons may be suppressed in external magnetic field leading to substantial changes of the dielectric permittivity in a broad frequency range.

DyMnO<sub>3</sub> belongs to the most studied multiferroic manganites with orthorhombic structure. Below the Néel phase transition at  $T = 39$  K DyMnO<sub>3</sub> first possesses an incommensurate magnetic order [15–17]. For  $T \leq 19$  K this order turns into a spin cycloid with the manganese spins rotating in the crystallographic  $bc$  plane. As has been proven both theoretically and experimentally, this spin structure leads to the occurrence of the static electric polarization parallel to the  $c$  axis [16, 18, 19]. Similar to such multiferroics like GdMnO<sub>3</sub> or TbMnO<sub>3</sub>, DyMnO<sub>3</sub> shows the series of electromagnons at finite frequencies, which basically consists of two modes at 2 and 6 meV (15 and 50 cm<sup>-1</sup>), respectively [13, 20, 21]. Although the physical mechanism of the electromagnons is not fully understood until now, the high frequency mode seems to correspond to a zone boundary magnon [22, 23]. This magnon acquires electric dipole activity and becomes visible in the optical spectra as a result of the Heisenberg exchange mechanism combined with the cycloidal spin structure. The up-to-date situation with the low-frequency electromagnon is a bit more complicated. According to recent experimental results [24, 25] on the closely similar multiferroic TbMnO<sub>3</sub>, the low-frequency electromagnon corresponds to an eigenmode of the cycloidal spin structure [26] which becomes infrared active due to an incommensurate spin modulation of the cycloid. We note that an alternative explanation based on anisotropic effects has been suggested as well [27, 28].

In this work we present the comparison of the electromagnon dynamics in external magnetic fields with the changes in the static dielectric permittivity in the multiferroic DyMnO<sub>3</sub>. Substantial decrease of the electromagnon frequency is observed in the cycloidal magnetic phase. This softening behavior correlates with an increase of the static dielectric permittivity, thus revealing similar dependence as predicted by the Lyddane-Sachs-Teller relation.

## EXPERIMENTAL DETAILS

The spectroscopic experiments in the terahertz frequency range ( $3 \text{ cm}^{-1} < \nu < 40 \text{ cm}^{-1}$ ) have been carried out in a Mach-Zehnder interferometer arrangement [29, 30] which allows measurements of the amplitude and the phase shift in a geometry with controlled polarization of radiation. Dynamic dielectric properties  $\varepsilon^*(T, B) = \varepsilon_1 + i\varepsilon_2$  were calculated from these quantities using the Fresnel optical equations for the complex transmission coefficient. The experiments in external magnetic fields up to 8 T have been performed in a superconducting split-coil magnet with polypropylene windows. A frequency-response analyzer (Novocon-

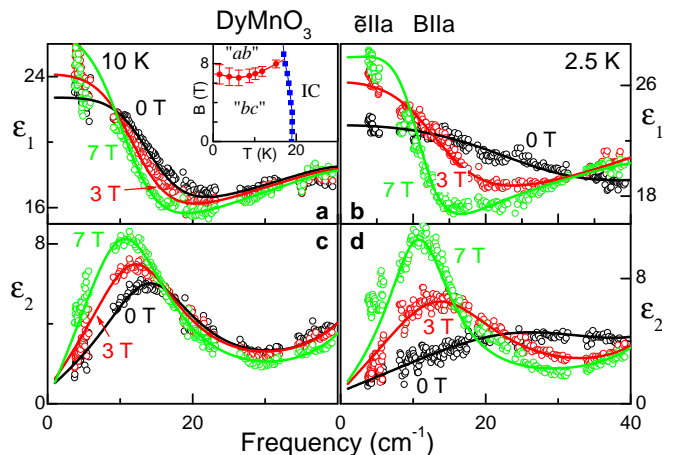


FIG. 1: Frequency dependence of the real (a,b) and imaginary (c,d) parts of the dielectric permittivity  $\varepsilon^* = \varepsilon_1 + i\varepsilon_2$  of DyMnO<sub>3</sub> along the  $a$  axis for different temperatures and external magnetic fields. For increasing magnetic fields a softening and a growth of intensity of the electromagnon is clearly observed. The inset shows the  $(B, T)$  phase diagram for static magnetic fields along the  $a$  axis. IC - incommensurate magnetic state, “ $ab$ ” and “ $bc$ ” denote the  $ab$ -plane and the  $bc$ -plane oriented cycloids, respectively. Error bars for the  $bc$ - $ab$  transition reflect the hysteresis and history dependence in different experiments.  $\vec{e}$  indicates the ac electric field of the electromagnetic wave.

trol alpha-analyzer) was used for static dielectric measurements. Single crystals of DyMnO<sub>3</sub> have been grown using the floating-zone method with radiation heating. The samples were characterized using X-ray, magnetic, dielectric and optical measurements [13, 31]. The results of these experiments including the magnetic phase diagrams are closely similar to the published results [16].

## RESULTS AND DISCUSSION

$$B \parallel a$$

Figure 1 shows typical spectra of the low frequency electromagnon in DyMnO<sub>3</sub>, which have been obtained in the magnetically ordered state with the spin cycloid oriented in the crystallographic  $bc$  plane. This phase is indicated as “ $bc$ ” in the phase diagram shown in the inset to Fig. 1. Application of an external magnetic field parallel to the crystallographic  $a$  axis leads to a rotation of the  $bc$  cycloid around the  $b$  axis from the  $bc$  plane to the  $ab$  plane. The spectra in Fig. 1 clearly demonstrate that in external magnetic fields  $B \parallel a$  the electromagnon shifts to lower frequencies and gains intensity. This behavior reveals already at this point a close similarity to classical soft modes. In order to investigate this similarity in more details, we have carried out the qualitative analysis of the electromagnon using the Lorentz-oscillator model

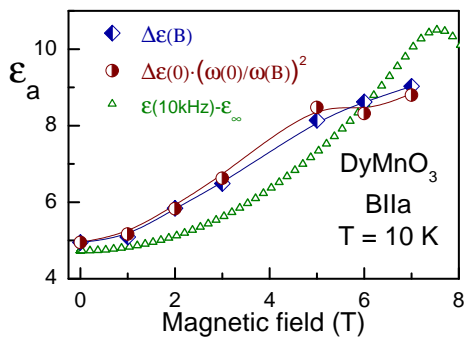


FIG. 2: Comparison of the static and dynamic properties of DyMnO<sub>3</sub> along the  $a$  axis. Diamonds represent the measured dielectric contribution of the electromagnon. Circles - dielectric contribution of the electromagnon as predicted by the LST relation. Triangles - static dielectric permittivity with a high-frequency value  $\epsilon_\infty = 25$  subtracted.

and compared these results with the static dielectric permittivity.

Figure 2 shows the magnetic field dependence of the dielectric contribution of the electromagnon in comparison with the static permittivity. Blue diamonds represent the field dependence of the dielectric contribution  $\Delta\epsilon$  of the low-frequency electromagnon showing an increase by more than a factor of two as approaching the phase transition to the  $ab$ -oriented spiral around 7 T. The dielectric contribution closely correlates with the decrease of the resonance frequency, which is demonstrated by plotting  $\Delta\epsilon \cdot \frac{\omega(0)^2}{\omega(B)^2}$  (red circles). This plot corresponds directly to the Lyddane-Sachs-Teller relation and reflects the conservation of the spectral weight of the electromagnon in external fields parallel to the  $a$  axis. Open triangles in Fig. 2 show the field dependence of the static dielectric constant in DyMnO<sub>3</sub> as measured at 10 kHz. Here we subtracted the contribution from the higher frequency processes ( $\epsilon_\infty = 25$ ) which is given by electronic transition, phonons, and a second electromagnon [20] at 6 meV. We observe a close correlation between static and dynamic properties in spite of more than seven orders of magnitude difference in frequency. According to the sum rules mentioned above, this result demonstrates that for the geometry  $B||a$  the changes in the static properties are nearly completely governed by the softening of the electromagnon and no other contributions exist between kHz and THz frequencies.

We note that a correspondence of lattice soft modes and electromagnons is not straightforward. The latter are defined in the ordered state and reveal critical behavior approaching a phase transition as function of magnetic field. The LST-derived equation for DyMnO<sub>3</sub> relates the dielectric constant at zero magnetic fields to that in finite fields, while it relates transverse and longitudinal modes in dielectrics. The softening of the electromagnon in external fields can be qualitatively under-

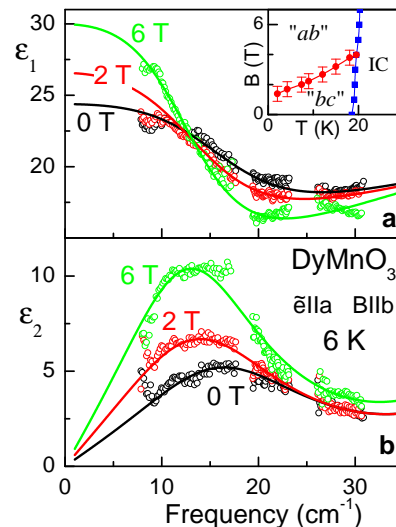


FIG. 3: Frequency dependence of the real (a,b) and imaginary (c,d) parts of the dielectric permittivity of DyMnO<sub>3</sub> for  $\vec{e}||a$  for different external magnetic fields  $B||b$  and at  $T = 6$  K. The inset shows the (B,T) phase diagram for static magnetic fields along the  $b$  axis. Notations are the same as in Fig. 1.

stood taking into account the switching of the orientation of the spin cycloid. Similar to many other structural transitions the effective stiffness of the cycloid probably tends to zero on the phase border between the  $bc$ - and  $ab$  cycloids, leading to a softening of the electromagnon. The unresolved question is: why the spectral weight of the electromagnon is conserved during the softening of the eigenfrequency? In case of classical softening of the lattice vibration one normally argues that the spectral weight of the soft mode is directly connected to the total number of electrons in the material. In agreement with the charge conservation a constant spectral weight may be expected for soft phonons. In case of a magnetic cycloid the electromagnon gains the spectral weight as a result of a complex interplay of various mechanisms. Therefore, we cannot use the conservation of the magnetic moment as an argument, and the observed conservation of the spectral weight remains an actual problem.

$$B||b$$

We turn now to the experimental geometry in which the transition from the  $bc$ - to the  $ab$  cycloid is achieved by magnetic fields along the  $b$  axis. Although here some hints to a soft mode behavior could be detected as well, the results turned out to be more complicated to interpret. Figure 3 reveal the terahertz spectra of the electromagnon in this geometry. We note at this point that similar spectra for this field geometry have been obtained previously in Ref. [20]. Similar to the data in Fig. 1, the spectra in the geometry  $B||b$  reveal an increase of

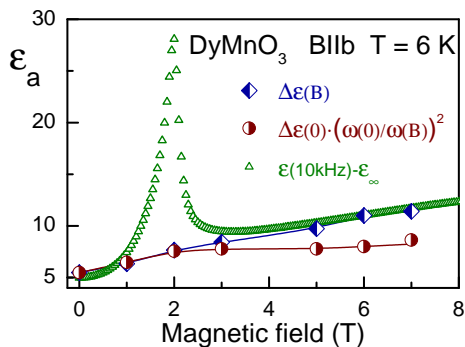


FIG. 4: Comparison of the static and dynamic properties of DyMnO<sub>3</sub> for  $\vec{e}||a$  and  $B||b$ . Diamonds represent the measured dielectric contribution of the electromagnon. Circles - dielectric contribution of the electromagnon as predicted by the LST relation. Triangles - static dielectric permittivity with a high-frequency value  $\varepsilon_\infty = 25$  subtracted.

the electromagnon intensity in external magnetic fields. However, already the comparison of the spectra at 6T and at 2T suggests that the increase of the mode intensity is not directly correlated with the decrease of the resonance frequency. Even without exact analysis of the fits one can see that the maxima in  $\varepsilon_2$  for 2T and 6T roughly coincide in spite of different intensities. Figure 4 presents the comparison of the static and dynamic properties for the geometry  $B||b$ . The electromagnon frequency in this geometry softens below 2T and then remains constant (red circles). Blue diamonds represent the strength of the electromagnon which increases continuously in the whole range of the magnetic fields investigated. Contrary to the results for the  $B||a$  (Fig. 2), above the transition to the  $ab$  cycloid at 2T the mode contribution  $\Delta\varepsilon$  deviates from the LST prediction  $\Delta\varepsilon \cdot \frac{\omega(0)^2}{\omega(B)^2}$  (red circles in Fig. 4). This reflects that the spectral weight of the electromagnon is not conserved in external fields  $B||b$ .

In addition, static dielectric constant as function of magnetic field is influenced by a second process which leads to the peak-like feature as documented in Fig. 4. Most probably, this feature has to be described using a different model. In this case we refer to the recent paper [32] by Kagawa *et al.* in which the dielectric contribution of the domain walls in DyMnO<sub>3</sub> has been investigated. It has been shown that the peak in the dielectric constant around  $bc$ -to- $ab$  phase transition is due to a domain wall relaxation with characteristic frequency situated in the radiowave range. We conclude that close to  $B = 2T$  the main changes in the static permittivity are due to the motion of the domain walls. However, except for the region close to 2T the overall increase of the static permittivity corresponds well to the dielectric contribution of the electromagnon. As a result, the similarity to the soft mode behavior is quite subtle for the  $B||b$  geometry. Here a better analogy is probably represented by the motion of the domain walls [32]. The relaxation rate of the

domain wall motion (Fig. 2 of Ref. [32]) seem to correlate well with the peak position of the static dielectric permittivity.

## CONCLUSIONS

The behavior of the electromagnon in DyMnO<sub>3</sub> in external magnetic fields has been investigated and compared to the changes of the static dielectric permittivity. A softening of the electromagnon is observed for external magnetic fields parallel to the  $a$ -axis, which is accompanied by an increase of the dielectric strength and of the static permittivity. Our results demonstrate that a soft-mode like behavior with a substantial increase of the static dielectric constant can be observed for electromagnons as well. In this case a magnetoelectric mode becomes soft and an external magnetic field serves as a driving parameter for this behavior. The observed similarity reveals further close connection between multiferroics and classical ferroelectrics. For magnetic fields parallel to the  $b$ -axis no direct correlation between the electromagnon frequency and the static dielectric permittivity exists. In this case the static properties seem to be governed by a motion of the domain walls.

## Acknowledgements

We acknowledge fruitful discussion with P. Lunkenheimer. This work was supported by DFG (Pi 372).

- 
- [1] R. Blinc and B. Žekš, *Soft modes in ferroelectrics and antiferroelectrics* (North-Holland Publishing, Amsterdam, 1974).
  - [2] W. Cochran, *Advances in Physics* **9**, 387 (1960), ISSN 0001-8732, URL <http://www.informaworld.com/10.1080/00018736000101229>.
  - [3] J. F. Scott, *Rev. Mod. Phys.* **46**, 83 (1974).
  - [4] J. Petzelt, G. V. Kozlov, and A. A. Volkov, *Ferroelectrics* **73**, 101 (1987), ISSN 0015-0193.
  - [5] R. A. Cowley, *Advances in Physics* **29**, 1 (1980), ISSN 0001-8732, URL <http://www.informaworld.com/10.1080/00018738000101346>.
  - [6] M. Dressel and G. Grüner, *Electrodynamics of Solids: Optical Properties of Electrons in Matter* (Cambridge University Press, Cambridge, 2002), 1st ed., ISBN 0521597269, URL <http://www.amazon.com/exec/obidos/redirect?tag=citeulike07->
  - [7] P. Lunkenheimer, U. Schneider, R. Brand, and A. Loidl, *Contemp. Phys.* **41**, 15 (2000), ISSN 0010-7514.
  - [8] N. Menon and S. R. Nagel, *Phys. Rev. Lett.* **74**, 1230 (1995).
  - [9] A. Pimenov, A. A. Mukhin, V. Y. Ivanov, V. D. Travkin, A. M. Balbashov, and A. Loidl,

- Nat. Phys. **2**, 97 (2006), ISSN 1745-2473, URL <http://dx.doi.org/10.1038/nphys212>.
- [10] M. Fiebig, J. Phys. D: Appl. Phys. **38**, R123 (2005), URL <http://stacks.iop.org/0022-3727/38/R123>.
- [11] Y. Tokura, Science **312**, 1481 (2006), <http://www.sciencemag.org/cgi/reprint/312/5779/1481.pdf>, URL <http://www.sciencemag.org>.
- [12] W. Eerenstein, N. D. Mathur, and J. F. Scott, Nature **442**, 759 (2006), ISSN 0028-0836, URL <http://dx.doi.org/10.1038/nature05023>.
- [13] A. Pimenov, A. M. Shuvaev, A. A. Mukhin, and A. Loidl, J. Phys.: Condens. Matter **20**, 434209 (2008), URL <http://stacks.iop.org/0953-8984/20/434209>.
- [14] A. B. Sushkov, M. Mostovoy, R. V. Aguilar, S.-W. Cheong, and H. D. Drew, J. Phys.: Condens. Matter **20**, 434210 (2008), URL <http://stacks.iop.org/0953-8984/20/434210>.
- [15] T. Kimura, S. Ishihara, H. Shintani, T. Arima, K. T. Takahashi, K. Ishizaka, and Y. Tokura, Phys. Rev. B **68**, 060403 (2003).
- [16] T. Kimura, G. Lawes, T. Goto, Y. Tokura, and A. P. Ramirez, Phys. Rev. B **71**, 224425 (2005).
- [17] R. Feyerherm, E. Dudzik, N. Aliouane, and D. N. Argyriou, Phys. Rev. B **73**, 180401 (2006).
- [18] S.-W. Cheong and M. Mostovoy, Nat. Mater. **6**, 13 (2007), ISSN 1476-1122, URL <http://dx.doi.org/10.1038/nmat1804>.
- [19] T. Goto, T. Kimura, G. Lawes, A. P. Ramirez, and Y. Tokura, Phys. Rev. Lett. **92**, 257201 (2004).
- [20] N. Kida, Y. Ikebe, Y. Takahashi, J. P. He, Y. Kaneko, Y. Yamasaki, R. Shimano, T. Arima, N. Nagaosa, and Y. Tokura, Phys. Rev. B **78**, 104414 (pages 9) (2008), URL <http://link.aps.org/abstract/PRB/v78/e104414>.
- [21] N. Kida, Y. Takahashi, J. S. Lee, R. Shimano, Y. Yamasaki, Y. Kaneko, S. Miyahara, N. Furukawa, T. Arima, and Y. Tokura, J. Opt. Soc. Am. B **26**, A35 (2009), URL <http://josab.osa.org/abstract.cfm?URI=josab-26-9-A35>.
- [22] R. V. Aguilar, M. Mostovoy, A. B. Sushkov, C. L. Zhang, Y. J. Choi, S.-W. Cheong, and H. D. Drew, Phys. Rev. Lett. **102**, 047203 (pages 4) (2009), URL <http://link.aps.org/abstract/PRL/v102/e047203>.
- [23] J. S. Lee, N. Kida, S. Miyahara, Y. Takahashi, Y. Yamasaki, R. Shimano, N. Furukawa, and Y. Tokura, Phys. Rev. B **79**, 180403 (pages 4) (2009), URL <http://link.aps.org/abstract/PRB/v79/e180403>.
- [24] A. Pimenov, A. Shuvaev, A. Loidl, F. Schrettle, A. A. Mukhin, V. D. Travkin, V. Y. Ivanov, and A. M. Balbashov, Phys. Rev. Lett. **102**, 107203 (pages 4) (2009), URL <http://link.aps.org/abstract/PRL/v102/e107203>.
- [25] A. M. Shuvaev, V. D. Travkin, V. Y. Ivanov, A. A. Mukhin, and A. Pimenov, Phys. Rev. Lett. **104**, 097202 (2010).
- [26] D. Senff, N. Aliouane, D. N. Argyriou, A. Hiess, L. P. Regnault, P. Link, K. Hradil, Y. Sidis, and M. Braden, J. Phys.: Condens. Matter **20**, 434212 (2008), URL <http://stacks.iop.org/0953-8984/20/434212>.
- [27] M. P. V. Stenberg and R. de Sousa, Phys. Rev. B **80**, 094419 (pages 5) (2009), URL <http://link.aps.org/abstract/PRB/v80/e094419>.
- [28] M. Mochizuki, N. Furukawa, and N. Nagaosa, Phys. Rev. Lett. **104**, 177206 (2010).
- [29] A. A. Volkov, Y. G. Goncharov, G. V. Kozlov, S. P. Lebedev, and A. M. Prokhorov, Infrared Phys. **25**, 369 (1985), ISSN 0020-0891, URL <http://www.sciencedirect.com/science/article/B6X3W-46K4CH2->
- [30] A. Pimenov, S. Tachos, T. Rudolf, A. Loidl, D. Schrupp, M. Sing, R. Claessen, and V. A. M. Brabers, Phys. Rev. B **72**, 035131 (2005).
- [31] F. Schrettle, P. Lunkenheimer, J. Hemberger, V. Y. Ivanov, A. A. Mukhin, A. M. Balbashov, and A. Loidl, Phys. Rev. Lett. **102**, 207208 (2009).
- [32] F. Kagawa, M. Mochizuki, Y. Onose, H. Murakawa, Y. Kaneko, N. Furukawa, and Y. Tokura, Phys. Rev. Lett. **102**, 057604 (2009).